Geopersia ***10*** *(2), 2020, PP. 367-380* *DOI: 10.22059/GEOPE.2020.288587.648501*

LA-ICP-MS zircon U-Pb geochronology on migmatites from the Boroujerd region, Sanandaj-Sirjan zone, Zagros Orogen, Iran: provenance analysis and metamorphic age

Seyedeh Razieh Jafari[1]*, Ali Asghar Sepahi[2], Yasuhito Osanai[3]

[1] *Department of Geology, Payame Noor University, PO BOX 19395-3697, Tehran, Iran*
[2] *Department of Geology, Bu-Ali Sina University, Hamedan, Iran*
[3] *Division of Earth Sciences, Kyushu University, Japan*
**Corresponding author, e–mail: sr.jafari2000@gmail.com*
(*received: 08/09/2019 ; accepted: 05/02/2020*)

Abstract

A narrow zone of migmatitic rocks forms part of the metamorphic complex associated with the Boroujerd plutonic complex in the north-western part of the Sanandaj-Sirjan zone, Iran. It includes stromatic, dyktionitic, schollen and massive migmatite, metatexites and diatexites. Leucosome (alkali-feldspar granitic and trondhjemitic) and mesosome are well developed, melanosome less so. Detrital zircon cores from one mesosome range in age from ~ 2540 to 210 Ma, with a major sub-population at ~ 250 Ma. The detrital zircon is probably derived from igneous bodies from the Iranian micro-plate (southern Eurasia) and possibly Pan-African and Arabian-Nubian basement no longer exposed. Metamorphism at 170–160 Ma recorded by thin metamorphic zircon rims is similar in age to the adjacent plutonic rocks from the Boroujerd area (172–169 Ma), both occurring in a middle Jurassic continental arc setting.

Keywords: *Geochronology, Migmatite, Boroujerd, Sanandaj-Sirjan Zone, Zircon.*

Introduction

Migmatites are a product of ultrametamorphism. Commonly, pelites and psammites metamorphosed under the conditions prevailing at the transition from upper amphibolite to granulite facies undergo partial melting to produce anatectic migmatite.

Migmatites occur near some of the plutonic complexes in the Sanandaj-Sirjan Zone (SSZ) of central western Iran, for example the complexes in the Boroujerd, Hamedan and Tueyserkan areas. Although many of the plutonic rocks in the zone, especially the granitic rocks, have been dated by U-Pb (e.g., Ahmadi Khalaji *et al.,* 2007; Shahbazi *et al.,* 2010; Ahadnejad *et al.,* 2011; Mahmoudi *et al.,* 2011; Azizi *et al.,* 2011; Esna-Ashari *et al.,* 2012; Chiu *et al.,* 2013; Azizi *et al.,* 2015; Yajam *et al.,* 2015), few ages have been measured on the migmatites and metamorphic rocks. Knowing the age of those rocks is key to determining the relationship between the igneous and metamorphic events and essential in interpreting the petrogenesis and geodynamic evolution of the SSZ and Zagros orogen.

The present study compares U-Pb ages newly-measured on metamorphic rocks from the SSZ with the results of previous dating of a variety of rocks, especially plutonic rocks, from both the region and adjacent areas. This provides a fresh perspective on the geological evolution of this poorly studied region.

Geological setting

The Sanandaj-Sirjan Zone, a metamorphic belt about 2000 km long containing various mafic, intermediate and felsic intrusive bodies (Fig. 1), is considered to be part of the Zagros Orogen (e.g., Alavi, 1994; 2004). Most of the metamorphism and magmatism in the SSZ occurred in the Mesozoic (e.g., Rashidnejad-Omran *et al.,* 2002; Sheikholeslami *et al.,* 2003; Baharifar, 2004; Ahmadi-Khalaji *et al.,* 2007; Sepahi *et al.,* 2014). The plutonic events in the north-western part of the SSZ are Mesozoic to Paleogene in age (e.g., Masoudi 1997; Ahmadi-Khalaji *et al.,* 2007; Shahbazi *et al.,* 2010; Mahmoudi *et al.,* 2011; Ahadnejad *et al.,* 2011; Azizi *et al.,* 2011; 2015; Esna-Ashari *et al.,* 2012; Chiu *et al.,* 2013; Sepahi *et al.,* 2014; Yajam *et al.,* 2015). Those events are considered to be the result of the subduction of Neo-Tethyan oceanic crust beneath the central Iranian micro-continent, and to later collisional/post-collisional tectonism (e.g., Baharifar, 2004; Sepahi *et al.,* 2004; 2014; 2018).

Migmatites occur in the vicinity of the Boroujerd Plutonic Complex (33˚38′–34˚00′ N, 48˚45′–49˚20’ E), a NW–SE trending intrusive body covering an area of nearly 600 km^2 in the NW SSZ (Fig. 1). That part of the SSZ is characterized by a predominance of metamorphic rocks and the

presence of granitoids. The Boroujerd Complex has field relationships, petrographic and geochemical features characteristic of metaluminous to slightly peraluminous, high-K calcalkaline, mainly I-type intrusions from active continental margins (Ahmadi-Khalaji *et al.,* 2007). The metamorphic rocks are mostly low- to high-grade metasedimentary rocks. A contact metamorphic sequence consisting of spotted schists, cordierite–andalusite and cordierite–sillimanite hornfelses extends to the NE of the pluton.

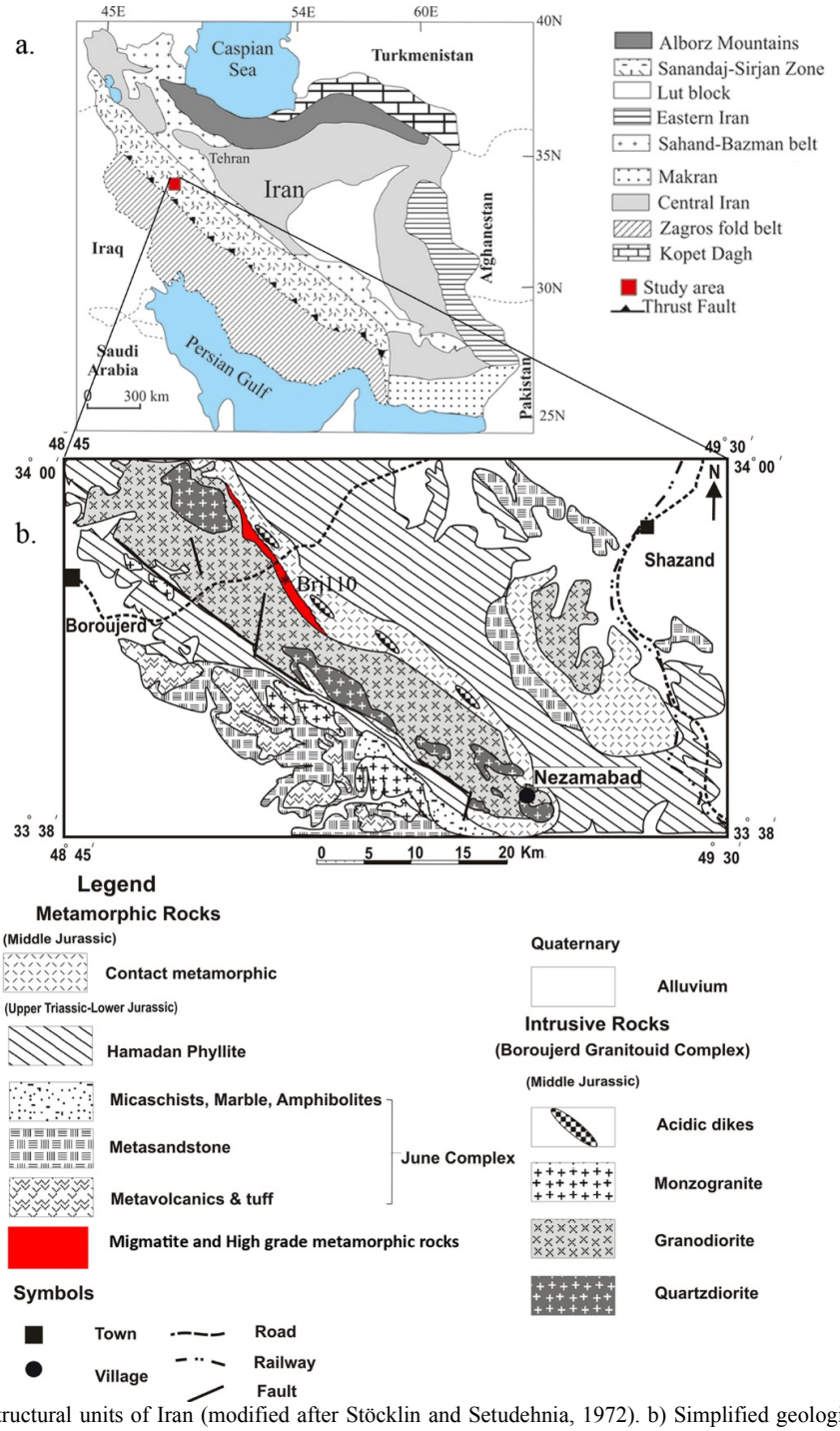

Figure 1. a) Major structural units of Iran (modified after Stöcklin and Setudehnia, 1972). b) Simplified geological map of the study area. The main rocks (intrusive and metamorphic) are shown (modified after Ahmadi-Khalaji *et al*., 2007).

The sedimentary protolith of the metamorphic rocks is considered to be middle Jurassic in age (Ahmadi-Khalaji *et al.,* 2007). Rb-Sr dating of plutonism and contact metamorphism in the region (Masoudi *et al.,* 2002; Masoudi & Yardly, 2005) has yielded ages ranging from early Cretaceous to Paleocene (130–52 Ma). Zircon U–Pb dating of granitoid rocks and associated pegmatitic dikes, however, has returned middle Jurassic ages of 172–169 Ma (Ahmadi-Khalaji *et al.,* 2007).

Petrography

Plutonic rocks

There are three main lithological units in the Boroujerd plutonic complex, 1) granodiorite, 2) quartz-diorite and 3) monzogranite, locally associated with felsic dikes (Ahmadi-Khalaji *et al.,* 2007).

The granodiorite is medium to coarse-grained. It is composed of plagioclase, biotite, quartz and alkali feldspar, with accessory apatite, zircon, allanite and opaque minerals. Some secondary muscovite is present.

The quartz-diorite occurs as small stocks with sharp contacts within the granodiorite. The rocks are equigranular to porphyritic, consisting of plagioclase, biotite, green amphibole, quartz and alkali feldspar. Accessory phases are zircon, titanite and apatite. Secondary minerals include sericite, epidote, chlorite, muscovite, opaque minerals, prehnite and calcite.

The monzogranite also occurs as small outcrops mainly through the southern part of the complex. The rocks have a fine to coarse grained granular texture in the central part of the unit, but are porphyritic at the margin. They are composed of quartz, alkali feldspar, plagioclase, biotite and secondary muscovite. Accessory phases are zircon, allanite and apatite.

There is a series of NW-SE trending aplites and pegmatites in the region. The aplites are composed of quartz, alkali-feldspar, some muscovite, tourmaline and opaque oxides. The pegmatites are characterized by the presence of quartz, feldspar, muscovite, tourmaline, zircon and apatite, with some andalusite and garnet in some samples.

Mafic dykes: These dykes are rare NE-SW trending features that crosscut the granodioritic unit. They are undeformed and contain amphibole, plagioclase, biotite, quartz, chlorite and epidote. Dismembered parts of some doleritic-gabbroic dykes are present as enclaves within the quartz diorites.

Felsic dykes: These dykes commonly have a NW-SE trend and crosscut the low- to medium-grade metamorphic rocks of the region. Most of the dykes are pegmatitic, but some are aplitic. The pegmatitic dykes are composed of plagioclase, quartz, K-feldspar, tourmaline, muscovite and rarely aluminosilicate minerals (sillimanite and andalusite) and garnet. The aplitic dykes commonly are layered—tourmaline-rich layers alternate with tourmaline-poor layers rich in mica, feldspar and quartz.

Metamorphic rocks:

The boundary between regional and contact metamorphic rocks in the Boroujerd region is not sharply defined. Far from plutons, slates and phyllites are common. Near the intrusions, spotted schists, hornfelsic schists, hornfelses and migmatites occur. The phyllites contain quartz, chlorite, muscovite (sericite), detrital feldspar, tourmaline and opaque minerals. The spots in the spotted schists, probably pseudomorphs after cordierite, are rich in micas (biotite, muscovite and chlorite) and occur within a fine-grained quartz- and sericite-rich matrix. The hornfelsed schists and hornfelses are commonly composed of cordierite, andalusite (chiastolite), sillimanite (fibrolitic, acicular and prismatic) and rarely garnet porphyroblasts in a matrix of quartz, feldspar and biotite. The andalusite porphyroblasts in some outcrops reach 100 mm in length. The cordierite and andalusite porphyroblasts are commonly rich in inclusions, mostly graphite and quartz. Minor tourmaline and muscovite are also present. The contact metamorphic grade in places has reached up to hornblende hornfels facies.

Migmatites

Near the Boroujerd complex, especially in the eastern part of the region, migmatitic rocks are exposed in the vicinity of Ghapanvari, Malmir, Khalaj, Sorkh-Dareh, Dodangeh and Hendodar (Fig. X). Structural forms in these rocks include stromatic (Fig. 2a), schollen (Fig. 2b-c), dyktionitic (Fig. 2d), nebulitic, and net structures. The migmatites exhibit various stages of partial melting, ranging from unmelted (Fig. 2e) to moderately melted (Fig. 2f), to highly melted and mobilized diatexitic granite (Fig. 2g).

Both leucosome and mesosome are common in the migmatites, but melanosome generally is not

well developed. There are some crosscutting felsic dykes and veins. Two types of leucosome are present: alkali-feldspar granitic and trondhjemitic. The former consists of alkali feldspar (commonly perthitic), quartz and muscovite (Fig. 3a). The latter is mainly quartz and plagioclase (sometimes with a myrmikitic texture), with accessory zircon (Fig. 3b).

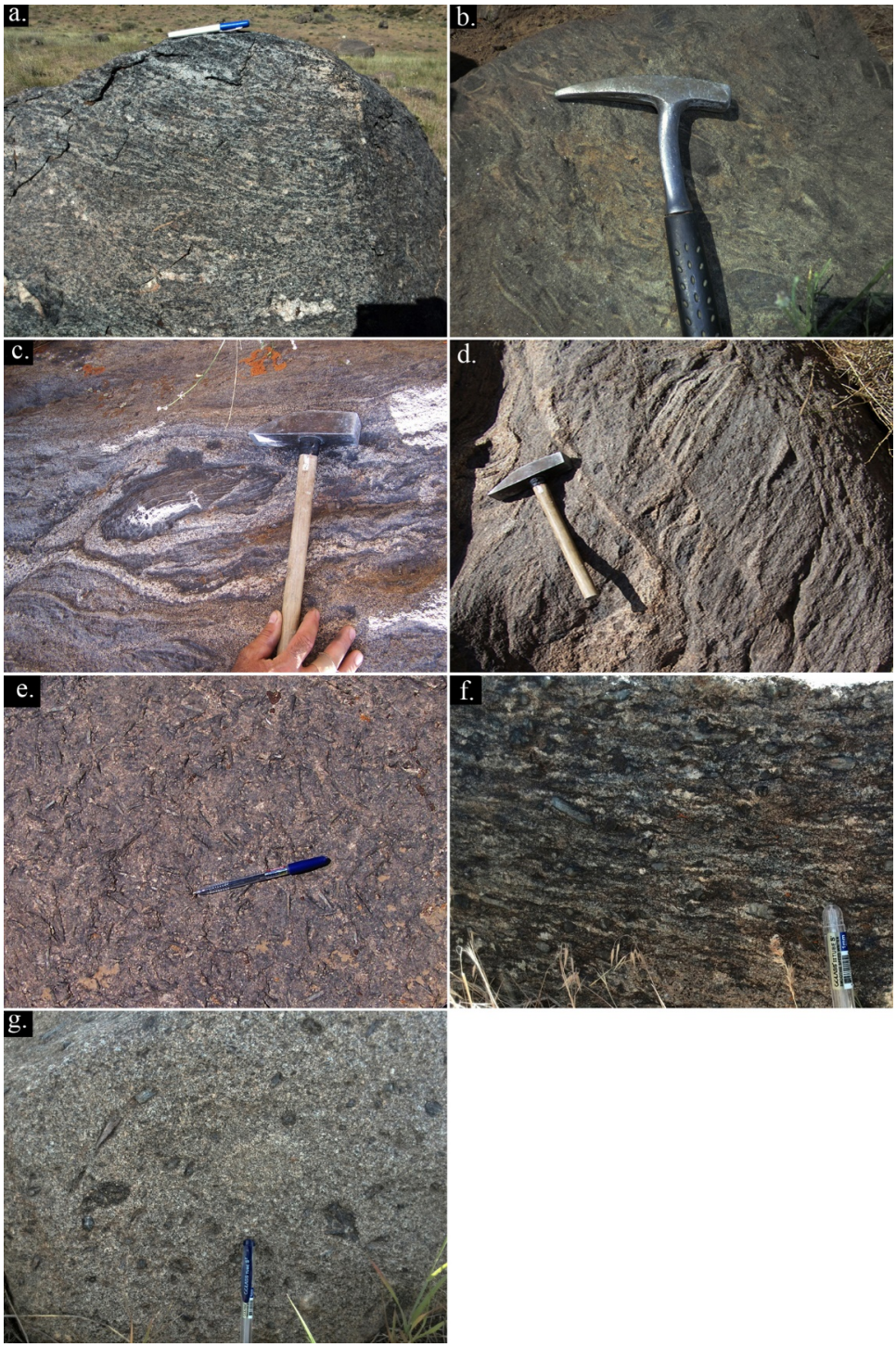

Figure 2. Selected outcrop photos of studied migmatites: a) Structure of stromatic, b-c) Structure of scholen, d) Structure of dyktionitic, e-g) Various stages of partial melting in migmatitic outcrops of the region: e) unmelted, f) moderately melted and g) highly melted.

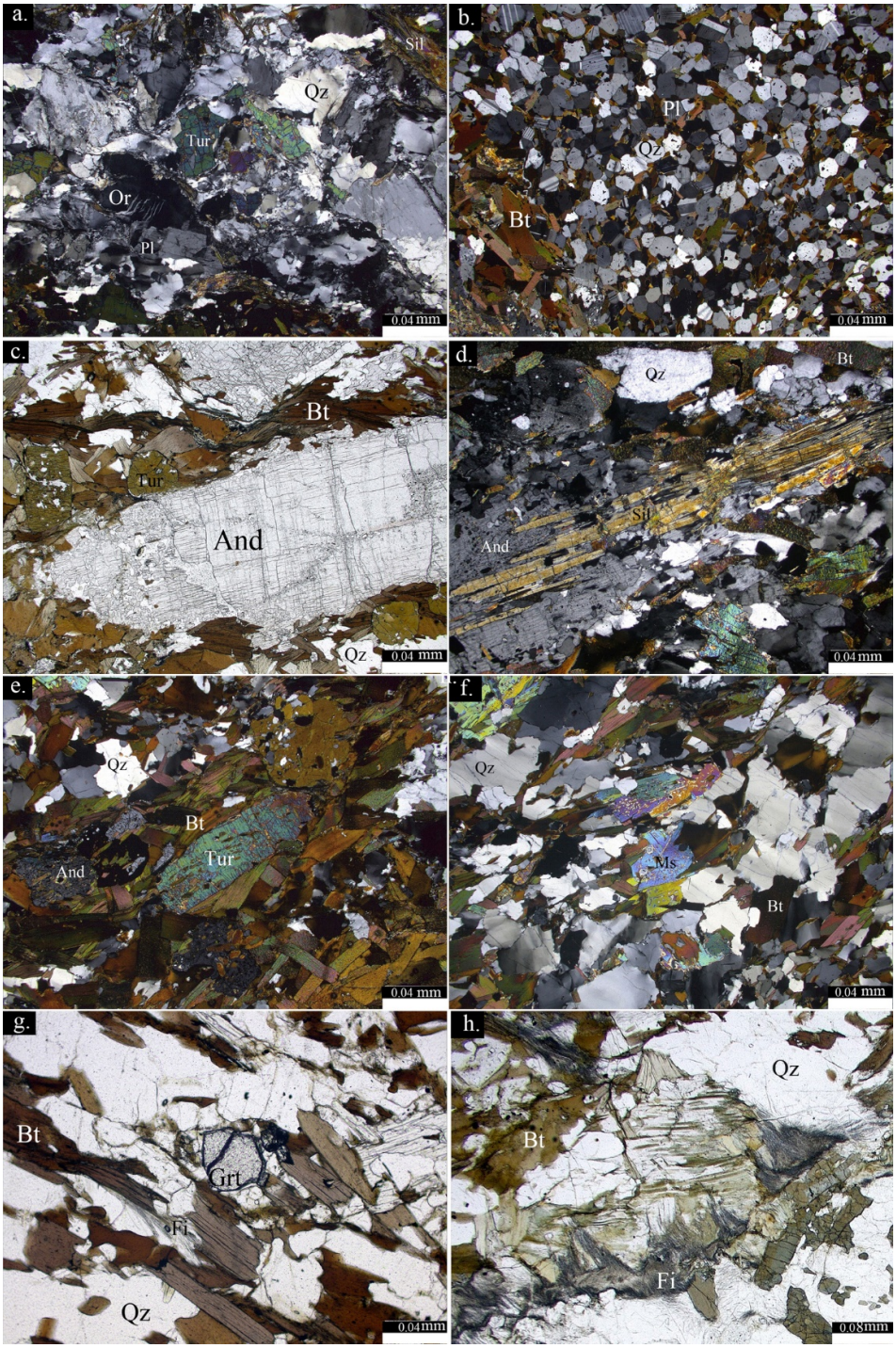

Figure 3. Photomicrographs of migmatites: a) K-feldspar-bearing leucosome, b) Plagioclase-bearing leucosome, c) porphyroblast of andalusite (chiastolite) contain graphite, quartz and biotite inclusions, d) sillimanite replacing andalusite, e) tourmaline existing in melanosome, f) secondary muscovite in migmatites of area, g) garnet in migmatites of area, h) fibrolite grow from mica. All mineral abbreviations used in figures are from Whitney and Evans (2010).
Qz= Quartz, And= Andalusite, Sil= Sillimanite, Or=Orthoclase, Pl=Plagioclase, Bt=Biotite.

Both types of leucosome contain minor biotite. The mesosome in the migmatites has a variety of textures (porphyroblastic, lepidoblastic, porphyro-lepidoblastic, poikilitic and symplectic) and mineralogy (andalusite, sillimanite, fibrolite, cordierite, muscovite, biotite, chlorite and

tourmaline) (Fig. 3c-e). Poikilitic porphyroblasts of andalusite contain inclusions of muscovite, biotite and quartz. Garnet is sometimes present, but rare (Fig. 3f). In some places fibrolite has formed at the expense of biotite (Fig. 3g). The metamorphism peaked at relatively low pressure and temperature, 400 MPa and 750 °C, respectively (Zare Shooli *et al.,* 2019).

Sample description, sample preparation, and analytical methods

Sample description

After a petrographic study of the migmatites, detrital zircon was separated from several samples and one sample of mesosome (Brj110) was chosen for U-Pb zircon geochronology. Brj110 contains quartz, orthoclase, plagioclase, garnet, andalusite/sillimanite, tourmaline-biotite, muscovite and zircon. The zircon is present as fine (up to 85 μm long), prismatic, subhedral to euhedral crystals with aspect ratios of 1.1–2.6.

Sample preparation, and analytical methods

Zircon was separated from the crushed rock using elutriation, magnetic separation and hand picking. Fifty-four spots representing 52 zircon grains from Brj110 were analyzed for U-Pb dating using an Agilent 7500cx quadrupole inductively coupled plasma mass spectrometer (ICP-MS) based on a New Wave Research UP-213Nd-YAG UV (213 nm) laser ablation system at Kyushu University, Japan.

The zircon grains were cast in epoxy discs and polished to expose the interiors of the crystals. Internal textures of the zircons were documented by cathodoluminescence (CL) imaging at Kyusho University using a JEOL JSM-5310S scanning electron microscope fitted with a Gatan Mini CL detector. This textural information was used to select the precise locations for the spot analyses. The size of analytical spots ranged from 30 to 80 μm.

The settings of the ICP-MS were optimized for maximum sensitivity using SRM-612 glass standard from the National Institute of Standards and Technology (NIST). The samples were ablated in a pure He (>99.99 vol. % He) atmosphere and transferred to the plasma torch mixed with pure Ar (> 99.99 vol. % Ar) gas.

The gas pipelines connected to the laser ablation chamber were mirror polished to maintain the ultra-high purity of the Ar gas and avoid air contamination. Because ^{204}Hg is an isobaric interference on ^{204}Pb, ^{202}Hg was monitored during the analyses. Both ^{202}Hg and ^{204}Pb were negligibly low during sample ablation, within the range of variation of the background (gas blank).

The raw isotopic data and the calibration of the zircon isotopic ratios were processed using GLITTER software (Griffin *et al.,* 2008) based on the analytical and calculating protocols for time-resolved LA-ICP analyses (Jackson *et al.,* 2004). The isotopic ratios measured on each analysed spot were checked and edited to omit the isotopically anomalous portion of each time profile using the procedures of Jackson and others (2004). The integrated isotopic ratios were calibrated against the Geoscience Australia standard zircon Temora 1 (Black *et al.,* 2003). Reference zircon FC-1 (Paces and Miller, 1993) was used as an internal calibration standard and as a secondary standard to ensure the accuracy of the isotopic ratios and calculated dates. The analytical uncertainty of individual analyses was calculated on the basis of the spot-to-spot reproducibility (2σ) of zircon FC-1, being typically 3.0% for ^{206}Pb/^{238}U and 3.5% for ^{207}Pb/^{235}U. Data calibrated against FC-1 were also tested in order to evaluate possible bias in the corrected values due to matrix effects related to differences in the chemical composition of the zircons. Concordia ages and diagrams were generated using Isoplot/Ex 3.0 software (Ludwig, 2003).

Results

Most of the zircon grains from Brj110 consisted of a large detrital core, commonly with oscillatory igneous zoning, surrounded by a homogeneous unzoned or mottled rim of metamorphic origin (Fig. 4). Such textures are common in zircon from high-grade metasedimentary rocks. The metamorphic rims were very thin, creating a risk, even when using a laser beam of only 30 μm diameter, of mixing signals from growth zones of different ages. Such mixing is unlikely, however—the detrital cores of the analyzed grains were so large that the possibility of spot overlap was very low, the two metamorphic rims chosen for analysis were both wide enough to be measured cleanly, and the editing function of GLITTER was used to select only data from homogeneous portions of the analysed volumes.

The measured U-Pb isotopic ratios and calculated dates for the analyzed zircon grains are listed in the Table 1.

Table1. LA-ICP-MS U-Pb isotope ratio and calculated age data of zircon from sample BRJ110.

Analysis No.	Isotopic ratios and errors (2σ)				Calculated ages and errors (Ma, 2σ)				Th/U
	$^{206}Pb/^{238}U$	error	$^{207}Pb/^{235}U$	error	$^{206}Pb/^{238}U$	error	$^{207}Pb/^{235}U$	error	
BRJ-1	0.0404	0.0014	0.2706	0.0162	255	8	243	13	0.66
BRJ-2	0.0683	0.0020	0.5400	0.0215	426	12	438	14	0.73
BRJ-3	0.0519	0.0016	0.3778	0.0168	326	10	325	12	0.12
BRJ-4	0.4823	0.0149	11.3946	0.4078	2537	65	2556	33	2.56
BRJ-5	0.1856	0.0053	1.9355	0.0673	1097	29	1093	23	0.42
BRJ-6	0.0413	0.0014	0.2933	0.0162	261	8	261	13	0.48
BRJ-7	0.3127	0.0125	4.6002	0.2546	1754	61	1749	46	0.88
BRJ-8	0.0462	0.0017	0.3661	0.0237	291	10	317	18	0.88
BRJ-9	0.1217	0.0044	1.2389	0.0720	740	25	818	33	2.08
BRJ-10	0.0715	0.0021	0.5500	0.0208	445	12	445	14	0.37
BRJ-11	0.0403	0.0012	0.2830	0.0118	255	7	253	9	1.20
BRJ-12	0.0426	0.0015	0.3163	0.0200	269	9	279	15	0.47
BRJ-13	0.1468	0.0044	1.3695	0.0535	883	25	876	23	1.08
BRJ-14	0.0823	0.0023	0.6958	0.0231	510	14	536	14	0.95
BRJ-17	0.2736	0.0102	3.6241	0.1889	1559	52	1555	41	1.00
BRJ-18	0.4402	0.0130	9.1267	0.3154	2351	58	2351	32	0.93
BRJ-20	0.0452	0.0013	0.3251	0.0140	285	8	286	11	0.40
BRJ-21	0.1575	0.0046	1.6767	0.0606	943	25	1000	23	0.22
BRJ-23	0.0561	0.0017	0.4176	0.0174	352	10	354	12	0.02
BRJ-24	0.0268	0.0008	0.1806	0.0094	171	5	169	8	0.04
BRJ-25	0.1129	0.0034	0.9694	0.0394	690	20	688	20	0.46
BRJ-26	0.1993	0.0062	2.1429	0.0904	1171	34	1163	29	0.07
BRJ-27	0.0860	0.0030	0.6850	0.0413	532	18	530	25	0.63
BRJ-28	0.1219	0.0038	1.0729	0.0487	742	22	740	24	0.33
BRJ-29	0.0652	0.0019	0.4909	0.0196	407	12	406	13	1.07
BRJ-30	0.4375	0.0126	8.9406	0.3040	2340	57	2332	31	0.18
BRJ-31	0.0340	0.0012	0.2383	0.0154	215	7	217	13	0.37
BRJ-32	0.2099	0.0060	2.9749	0.1040	1228	32	1401	27	0.10
BRJ-33	0.1226	0.0037	1.0836	0.0440	745	21	745	21	1.12
BRJ-34	0.0382	0.0012	0.2761	0.0141	242	8	248	11	2.59
BRJ-35	0.0963	0.0082	0.7937	0.2892	593	48	593	164	0.59
BRJ-36	0.1881	0.0064	1.9831	0.0969	1111	35	1110	33	0.04
BRJ-37	0.4163	0.0123	10.8088	0.3779	2244	56	2507	32	0.78
BRJ-38	0.4015	0.0120	7.4806	0.2687	2176	55	2171	32	0.89
BRJ-39	0.1055	0.0031	0.8920	0.0340	646	18	647	18	0.29
BRJ-40	0.0776	0.0032	0.6104	0.0558	481	19	484	35	0.64
BRJ-41	0.1124	0.0069	1.0817	0.1609	687	40	744	79	0.92
BRJ-42	0.1786	0.0051	1.8463	0.0660	1059	28	1062	24	0.35
BRJ-43	0.0403	0.0012	0.2926	0.0145	254	8	261	11	1.67
BRJ-44	0.0734	0.0025	0.6017	0.0344	457	15	478	22	0.49
BRJ-45	0.0809	0.0027	0.6330	0.0372	502	16	498	23	0.85
BRJ-46	0.1919	0.0056	3.8961	0.1386	1132	30	1613	29	0.30
BRJ-47	0.0900	0.0031	0.7291	0.0437	555	19	556	26	0.72
BRJ-48	0.1893	0.0055	2.0050	0.0732	1117	30	1117	25	0.27
BRJ-49	0.1560	0.0045	1.5002	0.0550	934	25	930	22	0.23
BRJ-50	0.1201	0.0043	1.0766	0.0636	731	25	742	31	0.62
BRJ-51	0.0338	0.0013	0.2368	0.0211	214	8	216	17	0.86
BRJ-52	0.0974	0.0029	0.8130	0.0326	599	17	604	18	0.51
BRJ-53	0.1388	0.0044	1.3100	0.0597	838	25	850	26	0.26
BRJ-54	0.1256	0.0038	1.1271	0.0483	763	22	766	23	0.15
BRJ-55	0.3158	0.0094	4.7591	0.1774	1769	46	1778	31	0.19
BRJ-56	0.0691	0.0020	0.5458	0.0220	431	12	442	14	0.21
BRJ-57	0.0257	0.0010	0.1735	0.0143	164	6	162	12	0.02
BRJ-58	0.3577	0.0123	6.1260	0.2703	1971	58	1994	39	0.26

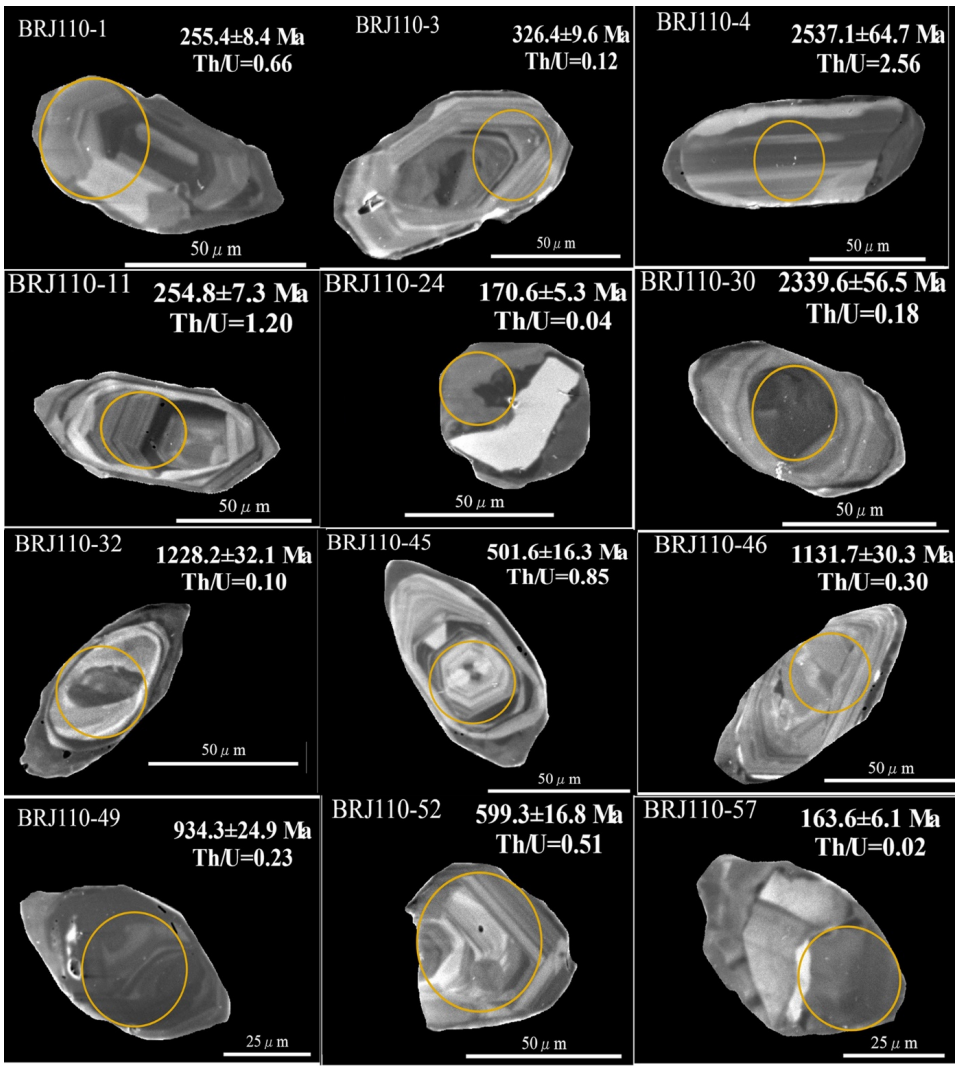

Figure 4. Selected CL images of zircon grains from Sample BRJ110.

The relationships between Th/U ratio and age are illustrated in Figure 5. The Th/U ratios range between 0.02 and 2.59. The mottled textured overgrowth domains with Th/U < 0.1 are metamorphic, while the majority of the cores, with remnant oscillatory or banded zoning and Th/U > 0.1 are igneous (e.g. Williams, 2001; Hoskin & Schaltegger, 2003; Rubatto, 2017). The U-Pb isotopic analyses are plotted in Figure 6 (a-c). Forty five analyses of detrital cores are concordant within analytical uncertainty, 7 are discordant. The two analyses of metamorphic rims are concordant (Fig. 6). The 206Pb/238U dates from the concordant cores range from ~ 2540 to 210 Ma, with distinct peaks at 2540, 2300, 2150, 1950, 1750, 1550, 1150, 750, 650, 400 and 250 Ma (Fig. 6d). The peak at 250 Ma is the strongest. The two rim analyses gave dates of 170–160 Ma (Fig. 6c).

Discussion

Comparison of the dates measured on the detrital zircon cores from mesosome Brj110 with previous U-Pb dating, especially of plutonic bodies in Iran, makes it possible to infer both the provenance of the cores and a possible heat source for the metamorphism.

Possible sources for detrital zircon cores (Neoproterozoic to pre-Jurassic plutons of Iran)

Determining the sources of the detrital cores of Archean to Mesoproterozoic age (>1000 Ma) is difficult because plutons with such ages have not been reported in Iran. Those cores are derived either from presently unexposed basement of the Iranian crust or other parts of ancient continents and supercontinents. Many plutons with pre-Jurassic ages (Neoproterozoic-Cambrian and younger) are

exposed in central Iran, and a few such plutons have also been reported from the SSZ and Alborz zone. These plutons might be the source of the detrital zircon cores with ages of 600–200 Ma, the most common component in the sample. The majority of these plutons are listed in Table 2.

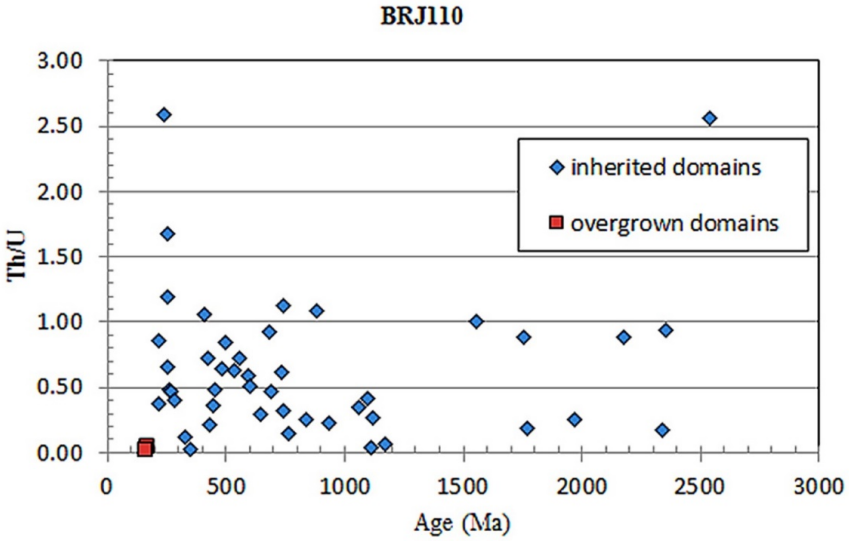

Figure 5. Th/U ratios versus zircon age of studied sample.

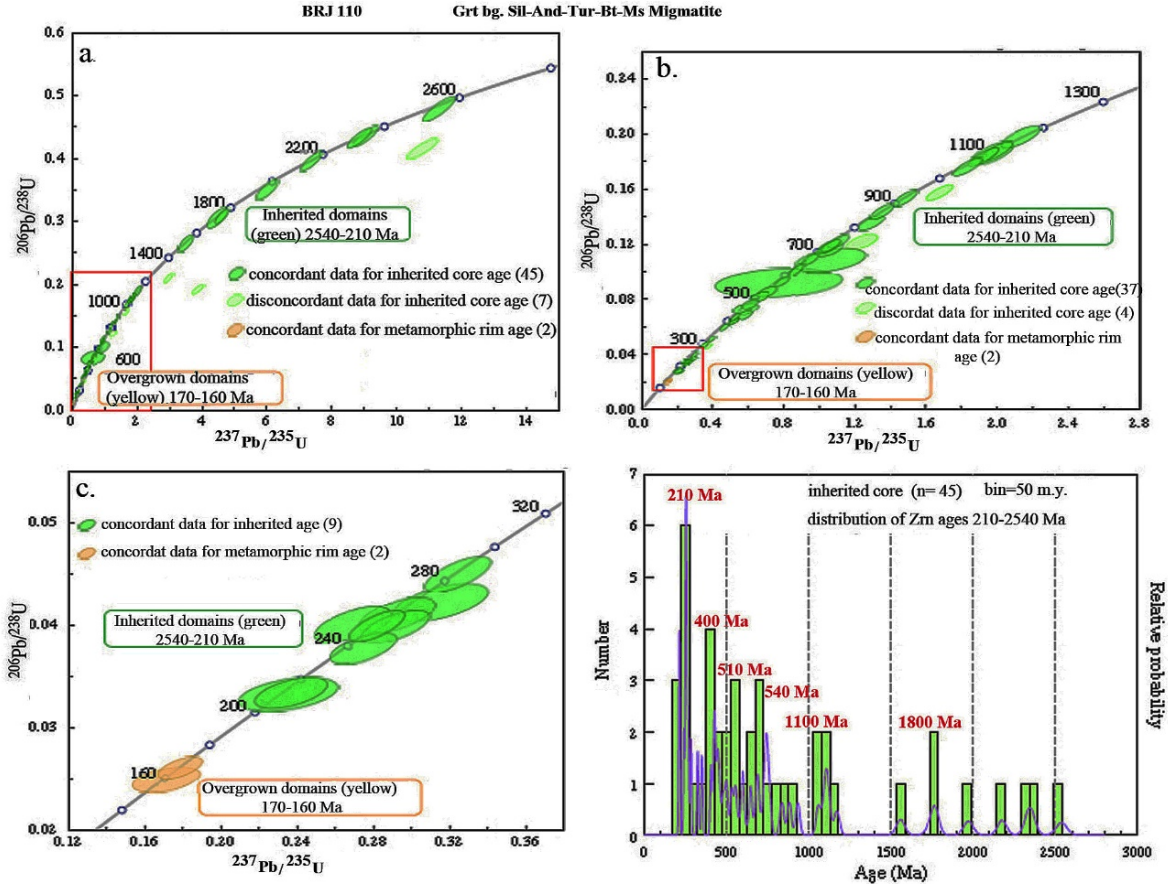

Figure 6. U/Pb Concordia diagrams, a-c: sample BRJ110 (a= for <2800 Ma, b= for <1300 Ma, c= for <320 Ma). d= Number/ relative probability versus age plot for inherited core of zircons for Sample BRJ110.

Table2. Age of major plutonic bodies of Iran.

Number	plutonic rocks name	Kind	Method	Age (Ma)	Location in Structural zone of Iran	eferences
1	Moghanlou	biotite-rich granitic orthogneiss	U-Pb	548 ± 27	CIR	Hassanzadeh *et al.* 2008
2	Mahneshan		U-Pb	568 ± 44	CIR	Hassanzadeh *et al.* 2008
3	Alborz	granite and orthogneiss		Neoproterozoic	AB	Hassanzadeh *et al.* 2008
4	Kouh-e Sefid Sang	biotite-garnet granodiorite	U- Pb	522 ± 23	CIR	Hassanzadeh *et al.* 2008
		leucocratic variety of the granite	U-Pb	534 ± 31 551 ± 20		
5	Alvand		U-Pb	165.1 ±2.0 & 163.9 ± 1.8	SSZ	Chiu *et al.* 2013
		porphyroid granite	K-Ar	81.8 ± 1.9		Baharifar *et al.* 2004
		pegmatite	k-Ar	74.7 ± 1.8		Baharifar *et al.* 2004
		quartz diorie	K-Ar	73.2 ± 3.1		Baharifar et al. 2004
		diorite	K-Ar	135.2 ± 3.1		Baharifar et al. 2004
		gabbro	U-Pb	166.5 ± 1.8		Shahbazi *et al.* 2010
		granite	U-Pb	163.9 ± 0.9 & 161.7 ± 0.6		Shahbazi *et al.* 2010
		leucogranite	U-Pb	154.4 ± 1.3 & 153.3 ± 2.7		Shahbazi *et al.* 2010
		norite	Rb-Sr	78-89		Valizadeh & Cantagrel 1975
		norite	K-Ar	89.1 ± 3		Valizadeh & Cantagrel 1975
		Pegmatite	Rb-Sr	104 ± 3		Valizadeh & Cantagrel 1975
		Pegmatite	K-Ar	82.8 ± 3		Valizadeh & Cantagrel 1975
		porphyroid granite	Rb-Sr	68 ± 2		Valizadeh & Cantagrel 1975
		porphyroid granite	K-Ar	63.8-80.8 ± 3		Valizadeh & Cantagrel 1975
6	Alvand pluton	granites	U-Pb	~165	SSZ	Mahmoudi *et al.* 2011
7	Almogholagh	diorite	Rb-Sr	144 ± 17	SSZ	Valizadeh & Cantagrel 1975
8	Malayer pluton	granite	U-Pb	162-187	SSZ	Mahmoudi *et al.* 2011
9	Boroujerd	Quartz diorie	U-Pb	170.7 ± 1.6	SSZ	Ahmadi-Khalaji *et al.* 2007
		Granodiorite	U-Pb	169.6 ± 0.2	SSZ	Ahmadi-Khalaji *et al.* 2007
				171.3 ± 1.1	SSZ	
				170.7 ± 1	SSZ	
		Monzogranite	U-Pb	171.7 ± 1.5	SSZ	Ahmadi-Khalaji *et al.* 2007
		pegmatite	U-Pb	170.7 ± 1.5	SSZ	Ahmadi-Khalaji *et al.* 2007
		Plutonic complex	U-Pb	~169	SSZ	Mahmoudi *et al.* 2011
		older granite	Rb-Sr	130 ± 1.4	SSZ	Masoudi 1997
		diorite	Rb-Sr	117.2 ± 1.2	SSZ	Masoudi 1997
		older pegmatite	Rb-Sr	127.3 ± 1.3 119.2 ± 1.3	SSZ	Masoudi 1997
		yanger granite	Rb-Sr	60-70 ± 0.7	SSZ	Masoudi 1997
		yonger pegmatite	Rb-Sr	52 ± 0.5	SSZ	Masoudi 1997
10	Qorveh pluton		U-Pb	157-149	SSZ	Mahmoudi *et al.* 2011
11	Aligoodarz	Granitoid complex	U-Pb	~165	SSZ	Esna-Ashari *et al.* 2012
12	Hasan-robat (near muteh)	Granite	U-Pb	288.3 ± 3.6	SSZ	Alirezaei & Hassanzadeh 2012
13	Band-e HezarChāh	granite	U-Pb	581±21	SSZ	Hassanzadeh *et al.* 2008
		orthogneisses		601±22		
14	Ariz	granite	U-Pb	533±1	CIR	Ramezani& Tucker 2003
15	Polo	granodiorite	U-Pb	530±21	CIR	Ramezani& Tucker 2003
16	Zarigan	leucogranite	U-Pb	525±7	CIR	Ramezani& Tucker 2003
17	Douzakh-Darreh	leucogranite	U-Pb	526±1	CIR	Ramezani& Tucker 2003
18	Sefid Granite	granite	U-Pb	525	CIR	Ramezani& Tucker 2003
19	Bubaktan	granodiorite	U-Pb	544 ± 19	SSZ	Hassanzadeh *et al.* 2008

20	Soursat Complex	granitoids	U-Pb	543± 6	SSZ?	Jamshidi-Badr *et al.* 2013
21	Muteh	granite	U-Pb	578±22 & 596±24	SSZ	Hassanzadeh *et al.* 2008
22	Haji Qara	orthogneisses	U-Pb	588±23	SSZ	Hassanzadeh *et al.* 2008
23	Lahijan	granite	U-Pb	551±9	AB	Hassanzadeh *et al.* 2008
24	Ghushchi complex	Granite & gabbronorites	U-Pb	320	AB	ShafaiiMoghadam *et al.* 2015
25	North Qorveh batholite		U-Pb	161±4	SSZ	Yajam *et al.* 2015
26	Shanevareh		U-Pb	160±2	SSZ	Yajam *et al.* 2015
27	Qalaylan		U-Pb	159±3	SSZ	Yajam *et al.* 2015
			U-Pb	157.9 ± 1.6 to 155.6 ± 5.6		Azizi *et al.* 2015
28	Galali		U-Pb	151±0.2	SSZ	Yajam *et al.* 2015
29	Saranjianeh		U-Pb	148±1	SSZ	Yajam *et al.* 2015
30	south Qorveh batholith		U-Pb	147±3	SSZ	Yajam *et al.* 2015
31	Bolbanabad-Havarpan		U-Pb	144±1	SSZ	Yajam *et al.* 2015
٣٢	Kolah Ghazi	granite	U-Pb	164.6±2.1	SSZ	Chiu *et al.* 2013
٣٣	Jiroft	granitoids	U-Pb	175.2±1.8	SSZ	Chiu *et al.* 2013
٣٤	Chah-Dozdan	granitoids	U-Pb	173–164	SSZ	Fazlnia *et al.* 2007

ZFT= Zagros Folded Thrust Belt, SSZ= Sanandaj-Sirjan zone, CIR= Central Iran, AB= Alborz-Azerbaijan zone.

On the basis of these ages for plutonic rocks and our data, the provenance of the detrital cores in the zircon grains is likely to be a range of different rocks (especially plutonic rocks) from various parts of ancient continents and supercontinents. The source of some zircons could be plutonic rocks of the Iranian micro-continent. Horton *et al.* (2008) reported inherited zircon grains from Iranian Phanerozoic sedimentary rocks with an age distribution of Mesoarchean (~ 3.0 Ga) to Miocene (<45 Ma). Their age distribution diagrams are dominated by zircon in the age range ~ 1000–500 Ma, but all contain a minor component that is much older, particularly ~2.6–2.4 Ga. They concluded that the zircon of ~ 900–600 Ma age was derived from a source region in East Africa (Pan-African basement). Zircon in young Phanerozoic orogenic belts can be inherited from much older sources, including older sediments.

Possible heat source for metamorphism (Jurassic plutons of the region?)

There is abundant evidence for Jurassic igneous activity in Iran. Chiu and others (2013) reported a U-Pb age of 164.6 ± 2.1 Ma for the Kolah Ghazi granite. In situ LA-ICP-MS zircon U-Pb dating of the Aligoudarz pluton yielded a crystallization age of ~ 165 Ma (Esna-Ashari *et al.,* 2012). Ahmadi-Khalaji *et al.* (2007) reported U-Pb zircon ages of 172–169 Ma for various samples of the Boroujerd pluton. U-Pb dating by Shahbazi and others (2010) has shown that a range of plutonic rocks within the Alvand pluton (Hamedan) were emplaced during the Jurassic: Gabbroic rocks 166.5 ± 1.8 Ma, granodiorites-monzogranites between 163.9 ± 0.9 and 161.7 ± 0.6 Ma, and leucocratic granitoids between 154.4 ± 1.3 and 153.3 ± 2.7 Ma. Mahmoudi and others (2011) obtained a similar age for this pluton. Two granite samples from the Alvand plutonic complex dated by Chiu and others (2013) gave zircon U-Pb ages of 165.1 ± 2.0 and 163.9 ± 1.8 Ma.

Mahmoudi and others (2011) determined a late Jurassic emplacement age for the Qorveh pluton (157–149 Ma) by the U-Pb dating method. The Suffiabad granite is exposed southeast of Sanandaj within the SSZ. LA-ICP-MS zircon U-Pb ages for this pluton range between 149 ± 2 and 144 ± 3 Ma (Azizi *et al.,* 2011). Yajam and others (2015) reported several SHRIMP U-Pb zircon ages in the range 160–140 Ma for plutons of the Qorveh region: north Ghorveh batholith 161 ± 4 Ma and Shanevareh 160 ± 2 Ma; Qalaylan 159 ± 3 Ma; central Ghorveh, Galali and Saranjianeh (151 ± 0.2 Ma to 148 ± 1 Ma); south Ghorveh batholith 147 ± 3 Ma and Bolbanabad-Havarpan 144 ± 1 Ma. The Ghalaylan pluton near Qorveh has yielded zircon U-Pb ages from 157.9 ± 1.6 to 155.6 ± 5.6 Ma (Azizi *et al.,* 2015). Granitoid rocks of possible Jurassic age have also been reported from several other areas in the SSZ, such as Jiroft (175.2 ±1.8 Ma; Chiu *et al.,* 2013), Chah-Dozdan (173–164 Ma; Fazlnia *et al.,* 2007).

These age ranges, especially those of plutonic rocks from the Boroujerd area, are close to the age obtained for the metamorphic rims of the zircon

grains from mesosome sample Brj110, 170–160 Ma. Some of the plutonic activity in the region was synchronous with the metamorphism. According to Sepahi (2008), the magmatism and metamorphism in the adjacent areas such as the Hamedan region occurred in a continental arc setting. According to this model, in such a setting metamorphism slightly predates plutonism but can subsequently be intensified by it. The metasedimentary protolith of the metamorphic rocks and migmatites possibly was deposited in a continental margin basin no older than Mesozoic at the southern edge of the Eurasia supercontinent. Detrital zircon in that protolith was transported from Late Archean to Mesozoic sources into that basin.

Conclusions

A narrow band of migmatitic rocks is present near the Boroujerd Plutonic Complex. A sample of mesosome from the Boroujerd area contains detrital zircon overgrown by thin metamorphic zircon rims. The detrital cores have a range of ages from late Archean (~ 2.54 Ga) to late Triassic (~ 210 Ma). Numerous sub-populations can be identified, the main one being ~ 600–250 Ma. The metamorphic zircon rims are Jurassic (~ 170–160 Ma), the same age as the igneous rocks from the Boroujerd region. The youngest group of detrital zircons (500–200 Ma) probably originated locally from the Iranian plate, whereas the older grains (> 2.5 Ga to 600 Ma) were possibly sourced from both northern Gondwana (e.g., the Arabian-Nubian Shield) and the neighboring, old cratons, perhaps Africa. The Neo-Tethys Ocean opened in the Permo-Triassic and closed in the middle Jurassic. The evolution of Neo-Tethys in the middle Jurassic and associated subduction beneath Iran caused extensive metamorphism and plutonism in the Sanandaj-Sirjan Zone of central western Iran. Magmatic activity, especially mafic plutonism at ~ 160 Ma, was the main trigger for the heat source of metamorphism, partial melting and migmatization. It can be associated with Jurassic magmatic pulses related to the subduction of the Neo-Tethyan oceanc lithosphere in the early to middle Jurassic.

Acknowledgement

We thank Lorence G. Collins and Ian Williams for editing the preliminary version of the manuscript.

References

Ahadnejad, V., Valizadeh, M.V., Deevsalar, R., Rezaei–Kahkhaei, M., 2011. Age and geotectonic position of the Malayer granitoids: Implication for plutonism in the Sanandaj–Sirjan Zone, W Iran. Neues Jahrbuch für Geologie und Paläontologie–Abhandlungen 261: 61–75.

Ahankoub, M., Jahangiri, A., Asahara, Y., Moayyed, M., 2013. Petrochemical and Sr–Nd isotope investigations of A–type granites in the east of Misho, NW Iran. Arabian Journal of Geosciences 6 (12): 4833–4849.

Ahmadi Khalaji, A., Esmaeily, D., Valizadeh, M.V., Rahimpour–Bonab, H., 2007. Petrology and geochemistry of the granitoid complex of Boroujerd, Sanandaj–Sirjan Zone, Western Iran. Journal of Asian Earth Sciences 29: 859–877.

Alavi, M., 1994. Tectonics of the Zagros orogenic belt of Iran: new data and interpretations Tectonophysics 229: 211–239.

Alavi, M., 2004. Regional stratigraphy of the Zagros fold–thrust belt of Iran and its proforeland evolution. American journal of Science 304: 1–20.

Alirezaei, S., Hassanzadeh, J., 2012. Geochemistry and zircon geochronology of the Permian A–type Hasanrobat granite, Sanandaj–Sirjan belt: A new record of the Gondwana break–up in Iran. Lithos 151:122–134.

Athari, S.F., Sepahi, A.A., Moazzen, M., 2007. Petrology of leucocratic granitoids of the northwest of Iran with emphasis on leucocratic I–type granites from the SW Saqqez, Neues Jahrbuch fuer Mineralogie–Abhandlungen 184(2): 169–179(11).

Asahara, Y., Mehrabi, B., Chung, S.L., 2011. Geochronological and geochemical constraints on the petrogenesis of high–K granite from the Suffi abad area, Sanandaj–Sirjan Zone, NW Iran Chemie der Erde–Geochemistry 71:363–376.

Azizi, H., Asahara, Y., Mehrabi, B., Chung, S.L. 2011. Geochronological and geochemical constraints on the petrogenesis of high–K granite from the Suffi abad area, Sanandaj–Sirjan Zone, NW Iran, Chemie der Erde – Geochemistry 71(4): 363–376.

Azizi, H., Zanjefili–Beiranvand, M., Asahara, Y., 2015. Zircon U–Pb ages and petrogenesis of a tonalite–trondhjemite–granodiorite (TTG) complex in the northern Sanandaj–Sirjan zone, northwest Iran: Evidence for Late Jurassic arc–continent collision Lithos 216–217: 178–195.

Baharifar, A., 2004. Petrology of metamorphic rocks in the Hamedan area, PhD, Tarbiat Moallem University of Tehran, Iran (in Persian).

Bea, F., Mazhari, A., Montero, P., Amini, S., Ghalamghash, J., 2011. Zircon dating, Sr and Nd isotopes, and element geochemistry of the Khalifan pluton, NW Iran: evidence for Variscan magmatism in a supposedly Cimmerian

superterrane. Journal of Asian Earth Sciences 40: 172–179.
Black, L.P., Kamo, S.L., Allen, C.M., Aleinikoff, J.N., Davis, D.W., Korsch, R.J., Foudoulis, C., 2003. TEMORA 1: a new zircon standard for Phanerozoic U–Pb geochronology. Chemical Geology, 200: 155–170.
Chiu, H–Y., Chung, S–L., Zarrinkoub, M.H., Mohammadi, S.S., Khatib, M.M., Iizuka, Y., 2013. Zircon U–Pb age constraints from Iran on the magmatic evolution related to Neotethyan subduction and Zagros orogeny. Lithos 162: 70–87.
Esna–Ashari, A., Tiepolo, M., Valizadeh, M.V., Hassanzadeh, J., Sepahi, A.A., 2012. Geochemistry and zircon U–Pb geochronology of Aligoodarz granitoid complex, Sanandaj–Sirjan zone, Iran. Journal of Asian Earth Sciences 43:11–22.
Fazlnia, A., Moradian, A., Rezaei, K., Moazzen, M., Alipour, S., 2007. Synchronous activity of anorthositic and S–type granitic magmas in Chah–Dozdan Batholith, Neyriz, Iran: evidence of zircon SHRIMP and monazite CHIME dating. Journal of Sciences, Islamic Republic of Iran 18: 221–237.
Griffin, W., Powell, W., Pearson, N., O'reilly, S., 2008. GLITTER: data reduction software for laser ablation ICP–MS in the earth sciences. Mineralogical Association of Canada short course series 40: 204–207.
Hassanzadeh, J., Stockli, D.F., Horton, B.K., Axen, G.J., Stockli, L.D., Grove, M., Schmitt, A.K., Walker, J.D., 2008. U–Pb zircon geochronology of late Neoproterozoic–Early Cambrian granitoids in Iran: implications for paleogeography, magmatism, and exhumation history of Iranian basement. Tectonophysics 451: 71–96.
Horton, B.K., Hassanzadeh, J., Stockli, D.F., Axen G.J., Gillis, R.J., Guest, B., Amini, A., Fakhari, M.D., Zamanzadeh, S.M., Grove, M., 2008. Detrital zircon provenance of Neoproterozoic to Cenozoic deposits in Iran: Implications for chronostratigraphy and collisional tectonics. Tectonophysics 451: 97–122.
Hoskin, P.W., Schaltegger, U., 2003. The composition of zircon and igneous and metamorphic petrogenesis. Reviews in mineralogy and geochemistry.53: 27 –62.
Jamshidi–Badr, M., Collins, A., Masoudi, F., Cox, G.M., Mohajjel, M., 2013. The U–Pb age, geochemistry and tectonic significance of granitoids in the Soursat Complex, Northwest Iran, Turkish Journal of Earth Sciences 22 (1):1–31.
Mahmoudi, S., Corfu, F., Masoudi, F., Mehrabi, B., Mohajjel, M., 2011. U–Pb dating and emplacement history of granitoid plutons in the northern Sanandaj–Sirjan Zone, Iran. Journal of Asian Earth Sciences 41: 238–249.
Masoudi, F., 1997. Contact metamorphism and pegmatites development in the region SW of Arak, Iran. PhD, University of Leeds, UK.
Masoudi, F., Yardley, B.W.D., Cliff R.A., 2002. Rb–Sr geochronology of pegmatites, plutonic rocks and a hornfels in the region south–west of Arak, Iran. Journal of Sciences, Islamic Republic of Iran 13(3): 249–254.
Masoudi, F., Yardley, B.W.D., 2005. Magmatic and metamorphic fluids in pegmatite development: Evidence from Borujerd Complex, Iran. Journal of Sciences, Islamic Republic of Iran. 16 (1): 43–53.
Nutman, A.P., Mohajjel, M., Bennett, V.C., Fergusson, C.L., 2014. Gondwanan Eoarchean–Neoproterozoic ancient crustal material in Iran and Turkey: zircon U–Pb–Hf isotopic evidence.Canadian Journal of Earth Sciences. 51: 272–285.
Paces, B.J., Miller, D.J., 1993. Precise UPb Ages of Duluth Complex and Related Mafic Intrusions, Northeastern Minnesota: Geochronological Insights to Physical, Petrogenetic, Paleomagnetic, and Tectonomagmatic Processes Associated With the 1.1 Ga Midcontinent Rift System. Journal of Geophysical Research. 98: 13997–14013.
Ramezani, J., Tucker, R.D., 2003. The Saghand region, Central Iran: U–Pb geochronology, petrogenesis and implications for Gondwana tectonics. American Journal of Science 303: 622–665.
Rashidnejad–Omran, N., Emami, M.H., Sabzehei, M., Rastad, E., Bellon, H., 2002. Lithostratigraphy and Paleozoic to Paleocene history of some metamorphic complexes from Muteh area, Sanandaj–Sirjan zone (southern Iran). Comptes Rendus Geosciences. 334 (16): 1185–1191.
Rubatto, D., 2017. Zircon: The Metamorphic Mineral. Reviews in Mineralogy and Geochemistry 83: 261–295.
Sepahi, A.A., Whitney, D., Baharifar, A., 2004. Petrogenesis of andalusite–kyanite–sillimanite veins and host rocks, Sanandaj-Sirjan metamorphic belt, Hamadan, Iran. Journal of Metamorphic Geology 22: 119–134.
Sepahi, A.A., 2008. Typology and petrogenesis of granitic rocks in the Sanandaj–Sirjan metamorphic belt, Iran: with emphasis on the Alvand plutonic complex. Neues Jahrbuch Fuer Geologie und Paleontologie–Abhandlungen 247(3): 295–312(18).
Sepahi, A.A., Shahbazi, H., Siebel, W., Ranin, A., 2014. Geochronology of plutonic rocks from the Sanandaj–Sirjan zone, Iran and new zircon andtitanite U–Th–Pb ages for granitoids from the Marivan pluton.Geochronometria 41: 207–215.
Sepahi, A.A., Jafari, S.R., Osanai, Y., Shahbazi, H., Moazen, M. 2018. Age, petrologic significance and provenance analysis of the Hamedan low–pressure migmatites; Sanandaj–Sirjan Zone, West Iran, International Geology Review 61(12):1446–1461.
Shafaii Moghadam, H., Li, X.H., Ling X.X., Stern, R.J., Santos, J.F., Meinhold, G., Ghorbani, G., Shahabi, Sh., 2015. Petrogenesis and tectonic implications of Late Carboniferous A–type granites and gabbronorites in NW Iran:

eochronological and geochemical constraints. Lithos 212–215: 266–279.
Shahbazi, H., Siebel, W., Pourmoafee, M., Ghorbani, M., Sepahi, A.A., Shang, C., Abedini, M.V., 2010. Geochemistry and U–Pb zircon geochronology of the Alvand plutonic complex in Sanandaj–Sirjan Zone (Iran): New evidence for Jurassic magmatism. Journal of Asian Earth Sciences 39: 668–683.
Sheikholeslami, R., Bellon, H., Emami, H., Sabzehei, M., Pique, A., 2003. New structural and 40K–40Ar data for the metamorphic rocks in Neyriz area (Sanandaj–Sirjan Zone, Southern Iran), Their interest for an overview of the Neo–Tethyan domain in the Middle East. Comptes Rendus Geoscience 335: 981–991.
Valizadeh, M.V., Cantagrel, J.M., 1975. Premières données radiométiques (K–Ar et Rb–Sr) sur les micas du complexe magmatique du Mont Alvand, près Hamadan (Iran occidental). Comptes Rendus Académie des Sciences 281, 1083–1086.
Yajam, S., Ghalamghash, J., Montero, P., Scarrow, J., Razavi, S., Bea, F. 2015. The spatial and compositional evolution of the Late Jurassic Ghorveh–Dehgolan plutons of the Zagros Orogen, Iran. Geologica acta 13:0025–0043.
Zare Shooli, M., Tahmasbi, Z., Saki, A., Ahmadi Khalaji, A., 2019. Mineral chemistry, pressure–temperature determination and fluids activities in Boroujerd migmatites using cordierite mineral, Iranian Journal of Crystallography and Mineralogy, 27 (1) :135–150.
Whitney, D.L., Evans, B.W., 2010. Abbreviations for names of rockforming minerals. Am Mineral 95:185–187.